Solid Freeform Fabrication 2018: Proceedings of the 29th Annual International Solid Freeform Fabrication Symposium – An Additive Manufacturing Conference
Reviewed Paper

NOT JUST NYLON… IMPROVING THE RANGE OF MATERIALS FOR HIGH SPEED SINTERING

R. Brown, C.T. Morgan, C.E. Majewski

Department of Mechanical Engineering, The University of Sheffield, Sheffield, S1 4BJ, UK

ABSTRACT

High Speed Sintering (HSS) is an emerging, recently commercialised Additive Manufacturing (AM) process which uses an infrared absorbing ink and infrared lamp to selectively sinter layers of polymer powder. Currently, Nylon 12 and its composites are used as the default feedstock due to their large processing windows. However, to meet the increasing variety of end use applications afforded by the benefits of AM, a wider range of materials must be developed. This work presents the characterisation and testing of a new elastomeric material for use in HSS. Parts were produced over a range of processing conditions, varying key parameters such as part bed temperature, ink density and lamp speed. Performance indicators including powder recovery, surface roughness and tensile data were evaluated over the range of conditions tested and all indicated the material's suitability for use as an HSS material.

INTRODUCTION

State of the industry

In recent years, improvements in reliability of machines and mechanical performance of parts have resulted in a rising interest in the use of AM for final part production [1]. However, many existing AM processes fail to meet the speed requirements needed to compete with traditional manufacturing techniques for series production runs exceeding 10,000 parts [2].

High Speed Sintering

High Speed Sintering is a recently commercialised polymer process which aims to address such productivity issues and ultimately become competitive with Injection Moulding. Selective sintering of a layer of polymer powder is achieved through ink-jet printing of an infrared absorbing ink, followed by irradiation with an infrared lamp, a schematic of which can be seen in Figure 1. Printed areas absorb more of the lamp energy than non-printed areas, causing sintering of the underlying powder [3]. Once sintering has occurred, a fresh powder layer is deposited and the process repeats. Throughout the build, the temperature of the part bed is maintained between the material's melt and recrystallisation temperatures to enhance layer-to-layer adhesion and prevent part warpage.

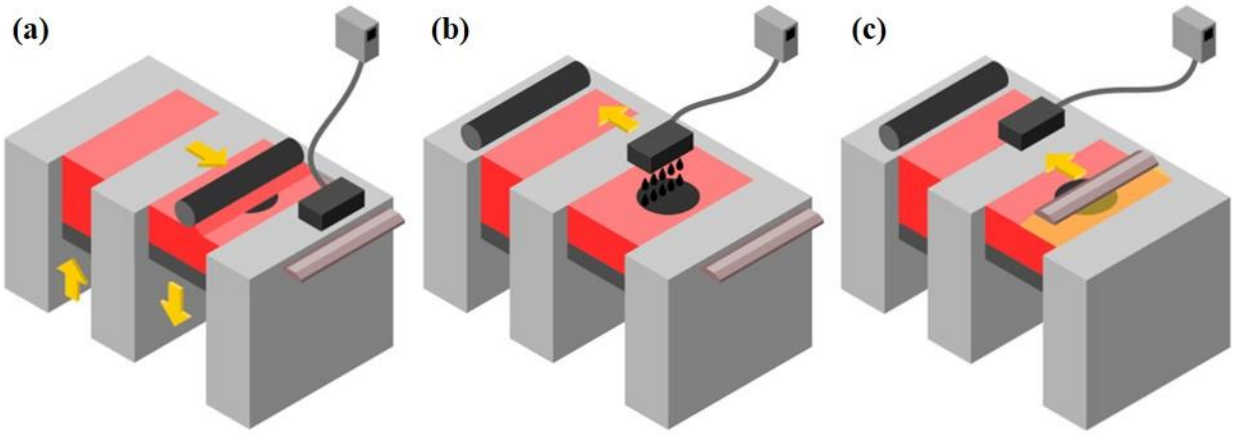

Figure 1 - HSS schematic illustrating (a) powder deposition, (b) ink deposition and (c) selective sintering of printed regions

Existing HSS research

Initial research into HSS focussed on optimising the process by identifying key parameters that influenced mechanical performance, with several studies concluding that part bed temperature, lamp speed and ink density all played an important role [4-6]. The majority of this research was conducted using Nylon 12 and its composites due to their large processing windows, enabling a wide range of parameters to be investigated. However, as more companies become interested in polymer sintering for a wider range of applications, demands for new, more diverse materials are emerging. One group of materials of interest are elastomers, which enable AM to expand into non-rigid applications such as the sports sector.

Currently, only one elastomeric material has been trialled in HSS - ALM's TPE210-S [7]. Whilst testing indicated that HSS could produce parts with excellent elongation at break, tensile strength was very low and parts had a poor surface finish, limiting use to out-of-sight and non-critical applications. The work presented here focusses on Eastman Chemical Company's Amphora^{TM} SP1621 thermoplastic elastomer, which has recently been released for the polymer sintering market.

METHODOLOGY

Parameter identification

Prior to part manufacture, the powder was characterised using Differential Scanning Calorimetry (DSC) to determine its thermal characteristics. A sample of approximately 20mg was heated from 20°C – 240°C at a rate of 10°C/min, before being cooled to 20°C at the same rate, producing the DSC trace seen in Figure 2. An initial part bed temperature of 180°C was selected in order to fall between the melt and crystallisation regions, as is standard practice for polymer sintering processes. All other initial parameters were selected based on their ability to successfully process materials previously trialled on HSS with similar melt enthalpies. A full list of the initial parameter settings used can be found in Table 1.

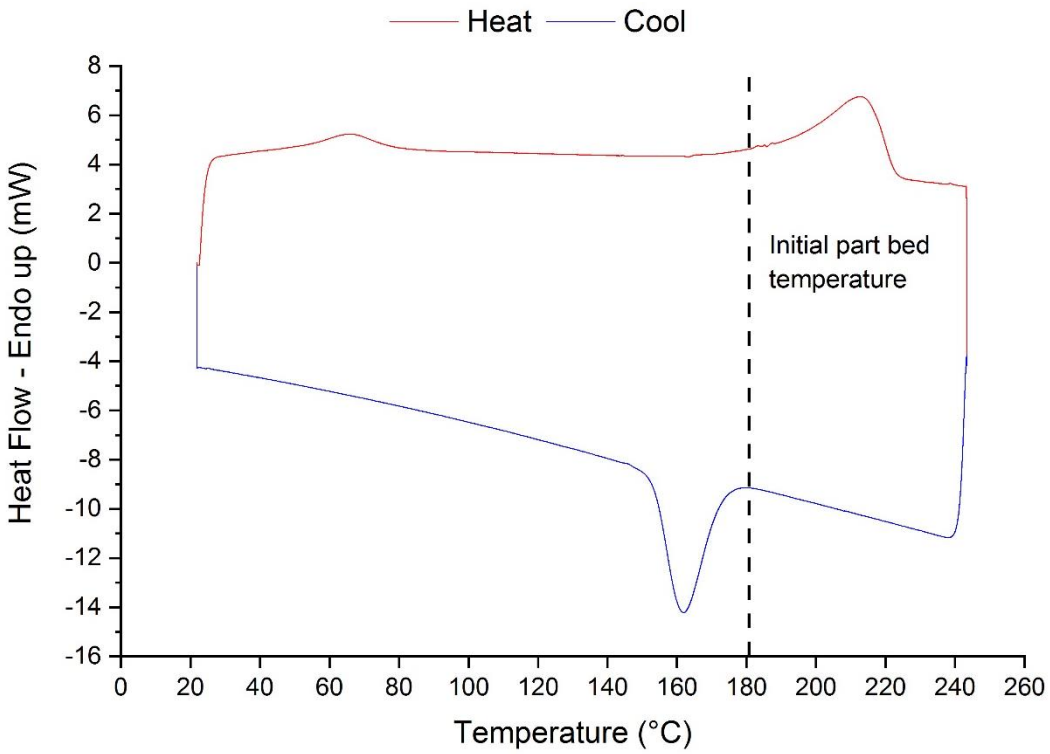

Figure 2 - DSC trace of Amphora™ SP1621

Table 1 - Initial parameter settings

Parameter	**Description**	**Initial setting**
Part bed temperature	Temperature at which the part bed is maintained throughout the build.	180°C
Recoat speed	Travel speed of the recoating carriage during powder deposition. Also the lamp's speed during preheating of the deposited powder.	70mm/s
Preheat lamp power	Percentage of maximum power supplied to the lamp to preheat recently deposited powder.	50%
Ink density	Quantity of ink deposited on the regions to be sintered. Quantified as the number of droplets that combine to form each dot deposited.	3 dots per drop
Lamp speed	Travel speed of the lamp during sintering of the printed regions.	80mm/s
Lamp power	Percentage of maximum power supplied to the lamp to sinter printed regions.	100%

Build setup

Six ASTM D638 type IV tensile specimens were arranged in the XY direction within the part bed, as shown in Figure 3. All parts were translated towards the front of the machine to compensate for a known temperature gradient across the part bed.

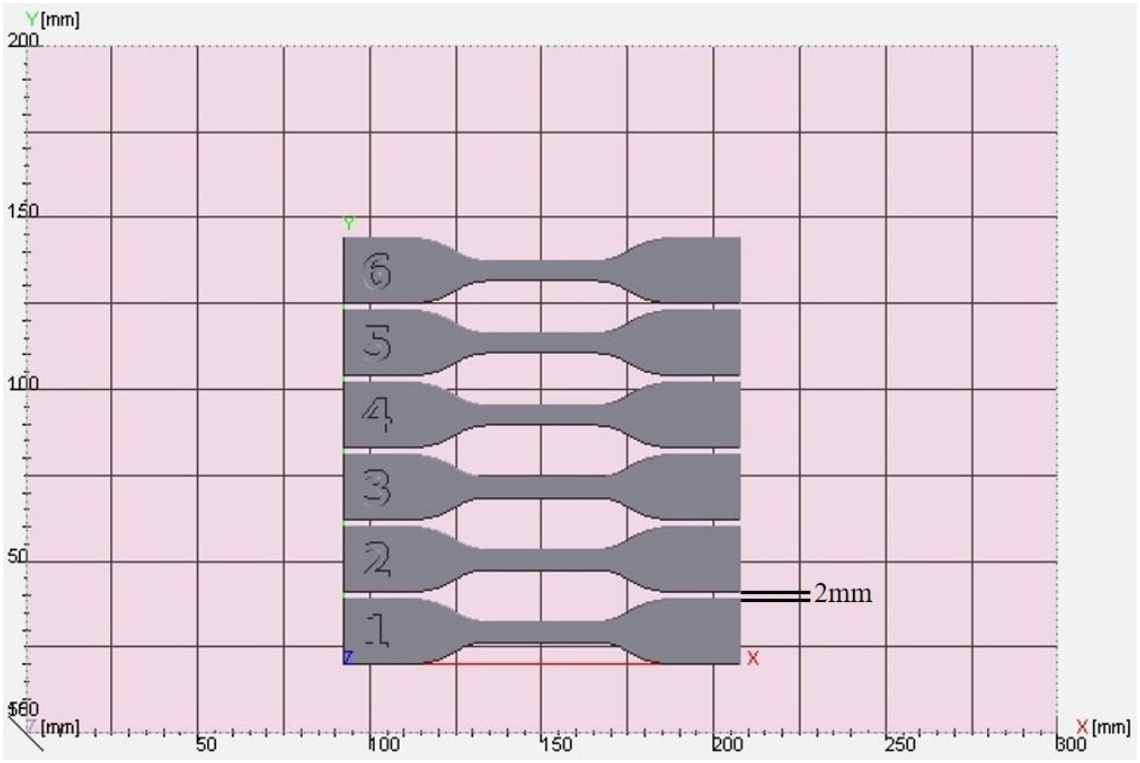

Figure 3 - Layout of tensile specimens within the part bed

Parts were manufactured using a voxeljet VX200 HSS prototype machine with virgin powder. Before each build, a 45-minute warm up period was conducted to raise the part bed to within 5°C of the target temperature, after which 50 blank layers were deposited to enable the temperature control system to accommodate the additional energy provided by the lamp. As the HSS process involves the lamp passing over the entire part bed, this also leads to some level of heating of the powder cake, increasing powder hardness [8]. As a result, build parameters must be carefully optimised to ensure any unused powder can be successfully recovered and sieved for re-use, whilst minimising the resulting decrease in mechanical performance.

Starting with the parameters listed in Table 1, the part bed temperature was decreased in 5°C increments per build until a build failed due to part warpage, or the parts could no longer survive post-processing. As there is often a tension between mechanical properties and powder removal in the HSS process, this enabled the identification of the best compromise.

Post-processing

Upon completion of a build, the part cake was immediately removed from the machine and left to cool to room temperature. Excess powder was removed where possible from the parts

using a scraper and collected along with any overflow powder for recycling. Both the re-useable powder (including overflow) and hard powder cake from each build were then weighed to estimate the percentage of powder that could be recovered for re-use. Following this, parts were bead-blasted to remove any remaining powder.

Surface profilometry

Surface profilometry was conducted on the top and bottom surfaces of each specimen to determine R_a, a measure of surface roughness, using a Mitutoyo Surftest SJ-400. Measurements were taken over an evaluation length of 4mm at 0.5mm/s, using a gaussian cut off filter of 0.8mm. Three measurements were taken on each surface and averaged for each specimen.

Tensile testing

Tensile testing was carried out using a Tinius Olsen H5KS in line with ASTM D638, using a grip separation speed of 5mm/min. Cross-sectional areas used to determine ultimate tensile strength and Young's modulus were calculated by averaging three width and thickness measurements taken along the gauge length of the specimens.

RESULTS & DISCUSSION

Effect of part bed temperature

Powder recovery

Table 2 shows how part bed temperature affected the ease with which parts could be separated from the powder cake and the proportion of unused powder that could be recovered for re-use. As expected, decreasing part bed temperature resulted in easier part/powder separation and an increase in the percentage of powder that could be recovered. This is due to a reduction in powder hardness resulting from a reduction in the overall energy supplied to the powder, as previously reported by both Majewski [4] and Thomas [8].

Table 2 - Variation of powder recovery with part bed temperature

Part bed temperature (°C)	Part breakout	Powder removal	% of powder recovered for re-use
180	Reduction of the powder cake to a rectangle around the parts.	Unable to separate parts through bead blasting.	59
175			57
170	Breakout of individual parts possible.	Incomplete powder removal.	77
165		Complete powder removal.	83
160			>99
155			>99
150	Build failed due to warpage.		

Whilst the inability to process above 170°C can be attributed to unwanted sintering of the part bed (supported by the long melt peak 'tail' in Figure 2), the ability to process the material below its recrystallisation temperature without inducing warpage is unusual. One possible explanation for this is that the degree of recrystallisation the material undergoes between layers is not significant enough to produce levels of shrinkage that result in part warpage.

Surface roughness

As can be seen from Figure 4, increasing part bed temperature appeared to initially reduce surface roughness, before sharply increasing at 170°C. This could be the result of improved particle melt until overheating results in poor powder removal, evidenced by Figure 5. The bottom surfaces of the specimens were also shown to be consistently smoother than the top. This has been previously observed in HSS, with some evidence to suggest this is due to the powder layer deposited immediately after the final layer of parts becoming embedded into the molten top surface [9].

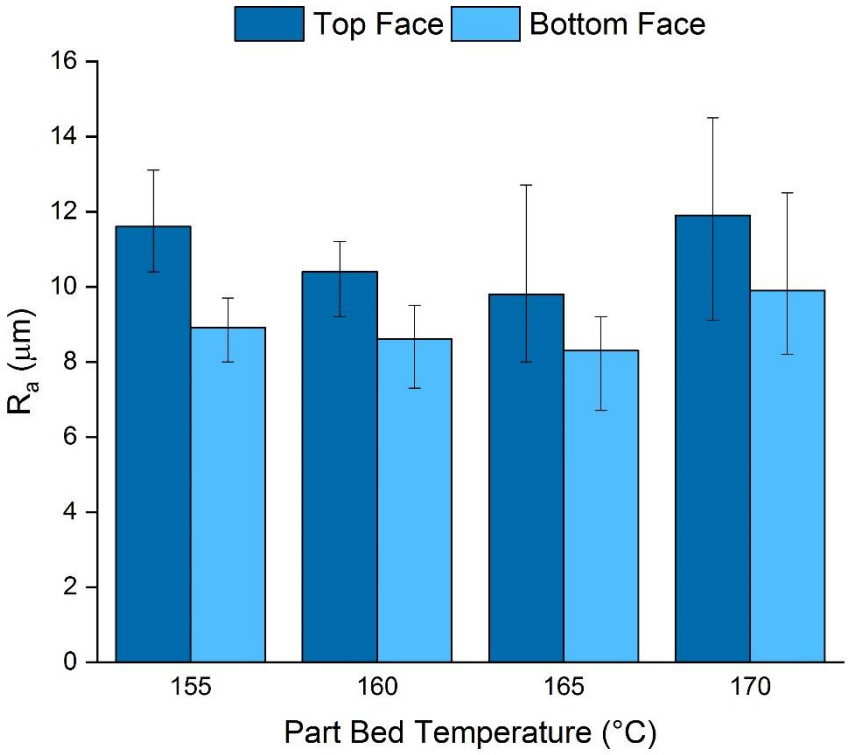

Figure 4 - Variation of surface roughness with part bed temperature

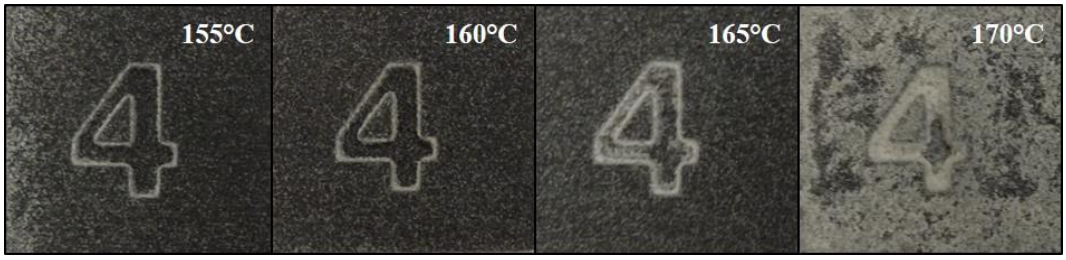

Figure 5 - Variation of top surfaces with part bed temperature (after bead-blasting)

Tensile properties

Figure 6 shows an increase in ultimate tensile strength, Young's modulus and elongation at break with part bed temperature. This can be explained by considering the increase in the total energy supplied to the parts, resulting in an increase in particle coalescence and densification, and has been previously demonstrated in both HSS and Laser Sintering [4, 10].

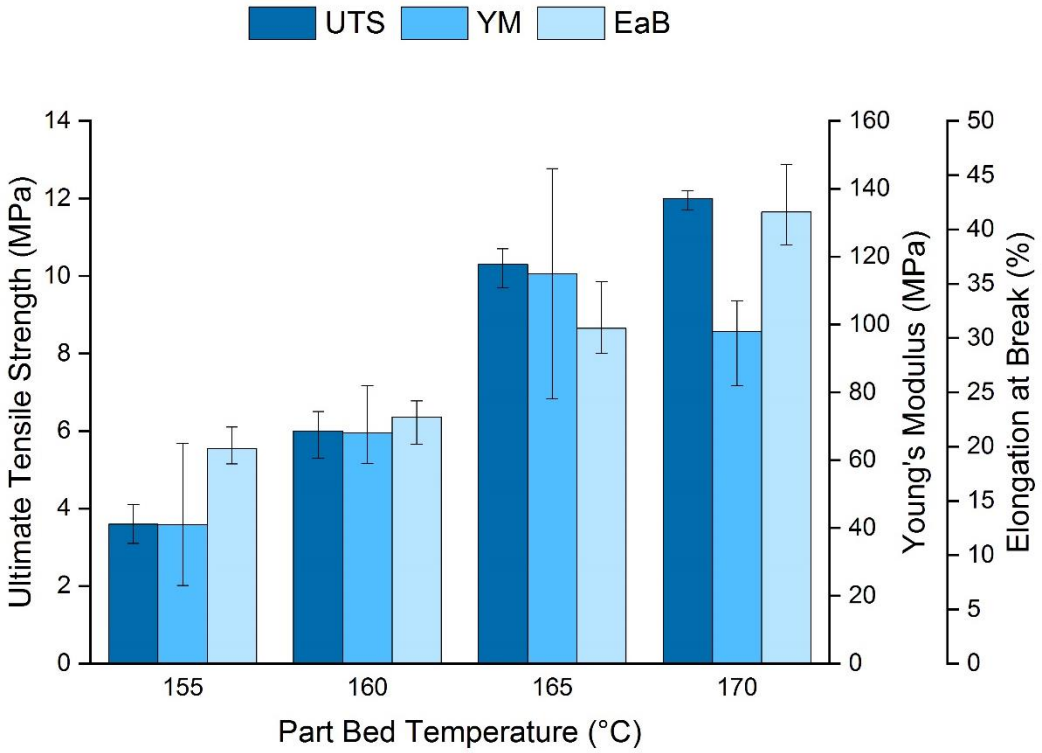

Figure 6 - Variation of tensile properties with part bed temperature

Effect of lamp speed

Using the results detailed in Table 2, an adjusted default part bed temperature of 160°C was selected for the remainder of the builds. This temperature was chosen to ensure a range of lamp speeds could be examined without risking part warpage or hindering powder removal. The default lamp speed of 80mm/s was subsequently increased and decreased by 20mm/s to investigate its effect on part production.

Powder recovery

Across the three lamp speeds tested (60, 80 and 100mm/s), little difference in the ability to post-process parts and recover powder for re-use was observed. In each case, individual parts could be broken out from the powder cake and all surrounding powder removed during bead-blasting. However, whilst both 100 and 80mm/s lamp speeds enabled maximum powder recovery, at 60mm/s unwanted powder bed sintering (≈3% of the total powder used) close to the parts was recorded. This can again be explained by considering that a slower lamp speed increases the total energy supplied to the powder, resulting in an increase in powder hardness, as

previously reported in the literature [4, 8]. Were additional lamp speeds to be tested, it would be expected that the percentage of powder viable for re-use would continue to decrease as speeds were reduced until only overflow powder could be recycled.

Surface roughness

As observed previously (Figure 4), Figure 7 shows that the bottom surfaces of parts manufactured were smoother than the top. Reducing the lamp speed also appeared to result in a slight reduction in top-surface roughness, similar to increasing part bed temperature. This apparent reduction may result from an increase in powder particle coalescence on the top face as more energy is supplied from the lamp. While not previously reported in HSS, a similar effect has been observed in Laser Sintering when an increased energy exposure time resulted in reduced surface roughness [11].

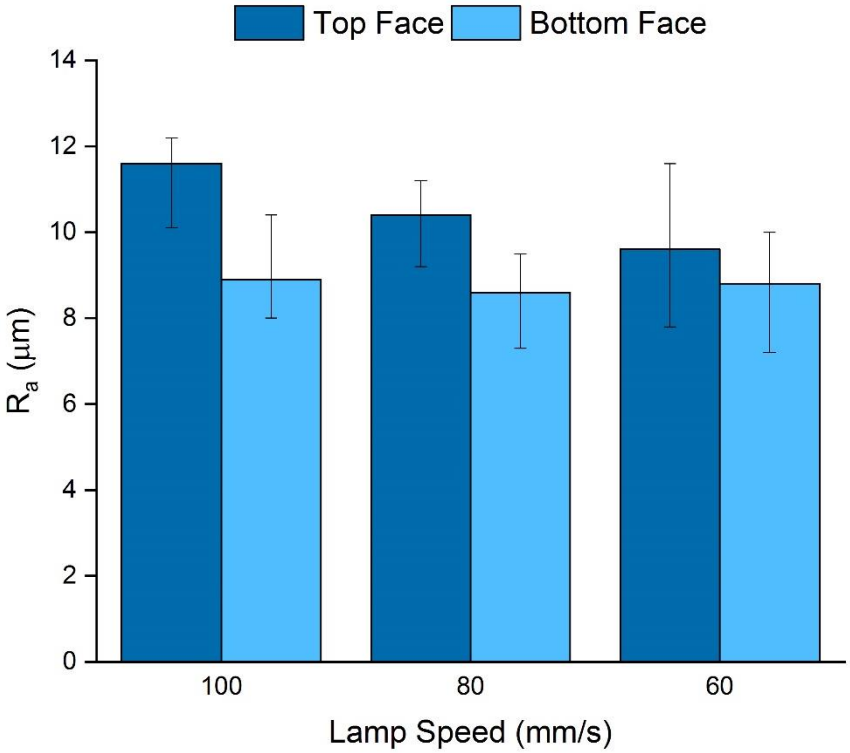

Figure 7 - Variation of surface roughness with lamp speed

Tensile properties

As with part bed temperature, lamp speed was shown to have a strong influence on tensile properties, with UTS, modulus and elongation at break all increasing as lamp speed decreased (see Figure 8). The increase in mechanical performance at lower lamp speeds can once again be explained by the increase in energy supplied, as previously demonstrated in HSS [4]. Reducing lamp speed in HSS is analogous to increasing energy density in Laser Sintering, which has also been shown to produce a similar effect [12].

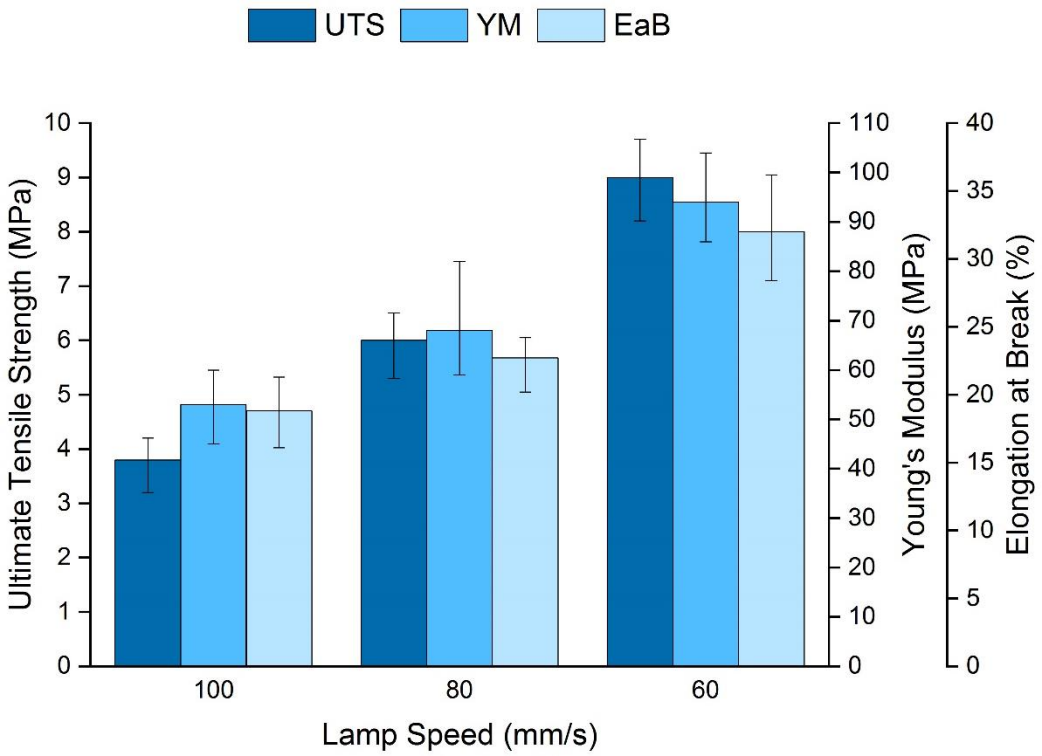

Figure 8 - Variation of tensile properties with lamp speed

Effect of ink density

Starting with the minimum possible for the standard printing array (each dot deposited comprising of a single droplet of ink), the ink density of subsequent builds was increased in increments of two, up to the maximum possible of seven drops per dot.

Powder recovery

Ink density was shown to have no effect on powder recovery, with each build performing as previously described in Table 2 at 160°C.

Surface roughness

Figure 9 shows that, similarly to part bed temperature, increasing ink density initially reduced top-surface roughness. At the highest level of ink density, a sharp increase in top-surface roughness was seen. The sudden increase again corresponded with a change in powder removal from the parts (Figure 10). As previously, bottom surfaces were shown to be smoother than the top surfaces of parts.

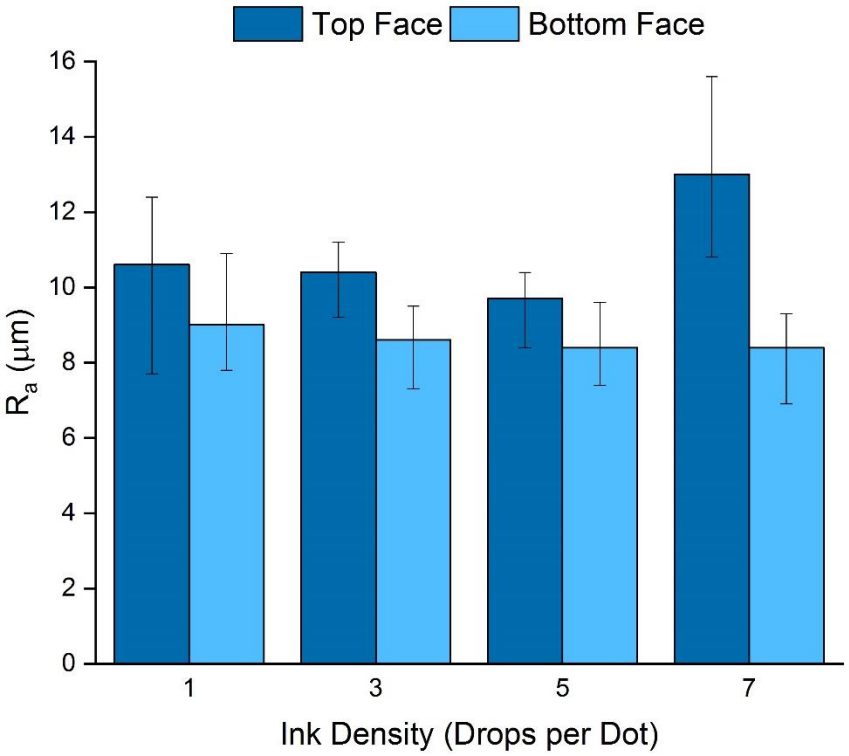

Figure 9 - Variation of surface roughness with ink density

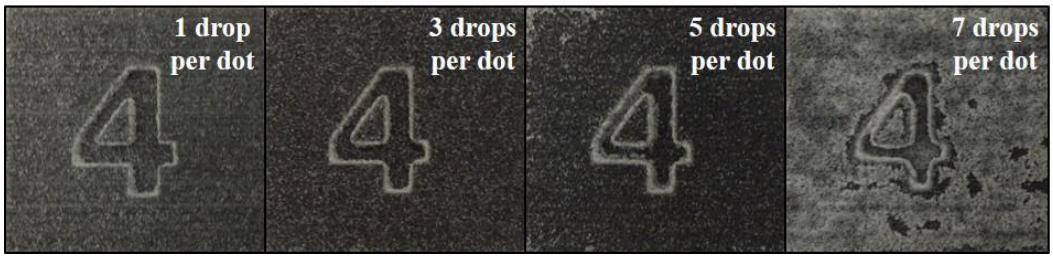

Figure 10 - Variation of top-face surfaces with ink density (after bead-blasting)

Tensile properties

Initial results from parts manufactured at ink densities of one, three, five and seven drops per dot indicated an optimum mechanical performance in the region of three drops per dot. As a result, additional builds were conducted at the remaining ink densities which confirmed a peak performance at three drops per dot, as seen in Figure 11. This behaviour has been previously observed in HSS for both elastomers and rigid polymers, with the initial increase in performance attributed to an increase in energy absorbed by the parts due to additional ink present [5, 6]. Whilst not confirmed, the subsequent decrease in performance at higher ink densities has been attributed to either thermal degradation of the polymer or inhibited sintering resulting from excess ink within the part. An alternative explanation could be that the cooling effect of the relatively cold ink (≈40°C) at higher ink densities outweighs the additional energy absorption from the ink, resulting in an overall decrease in the total energy supplied to the part.

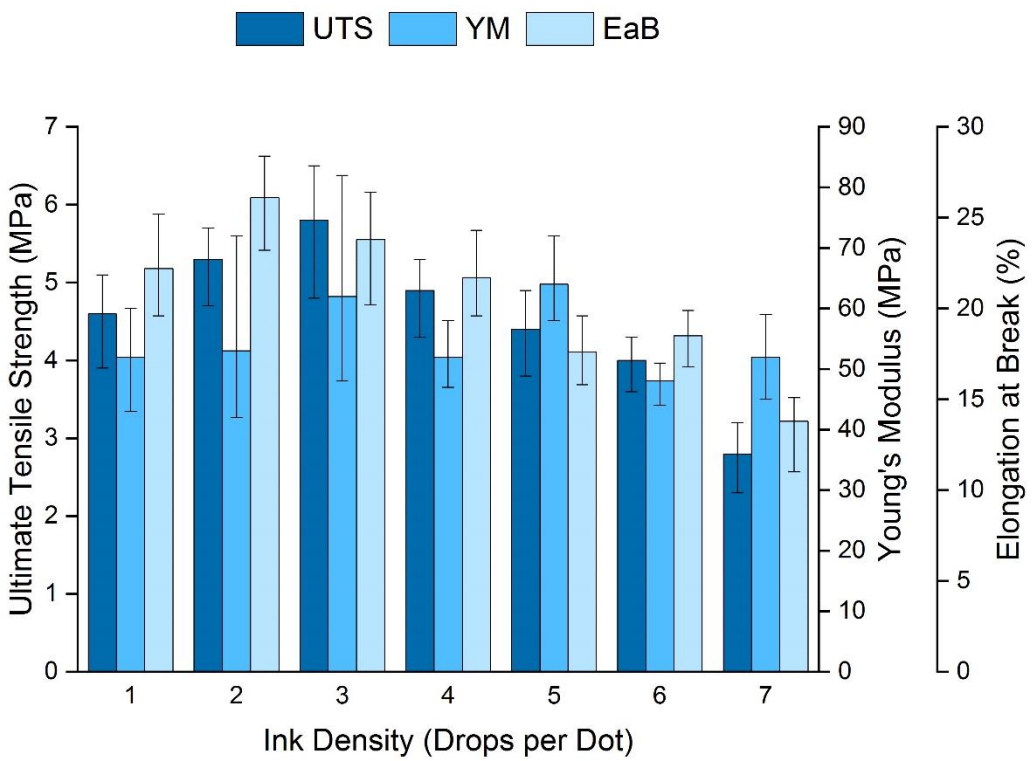

Figure 11 - Variation of tensile properties with ink density

CONCLUSIONS

This work has demonstrated the ability to process Amphora™ SP1621 in the High Speed Sintering process, over a wide range of processing parameters. In general, and similarly to Laser Sintering, an increase in energy input into the parts led to an increase in mechanical performance. Values of UTS and modulus were achieved which were comparable with quoted datasheet values [13] for Laser Sintering of this material. However, elongation at break was substantially lower than LS datasheet values, as a result of an inability to input sufficient energy into the parts without severely compromising powder removability. Further advances in the HSS technology, and in particular powder heating mechanisms, are likely to provide improvements in this area.

ACKNOWLEDGMENTS

This work was funded by the EPSRC (Grant: EP/L016281/1) as part of the Centre for Doctoral Training in Polymers, Soft Matter and Colloids. The author would like to thank the 3D Printing team at Eastman Chemical Company for supplying the material used for this work.

REFERENCES

[1] I. Wohlers Associates, Wohlers report 2018 : 3D printing and additive manufacturing state of the industry : annual worldwide progress report, Fort Collins, Colo. : Wohlers Associates, 2018, Fort Collins, Colo., 2018.

[2] M. Ruffo, C. Tuck, R. Hague, Cost estimation for rapid manufacturing - laser sintering production for low to medium volumes, Proceedings of the Institution of Mechanical Engineers, Part B: Journal of Engineering Manufacture 220(9) (2006) 1417-1427.

[3] N. Hopkinson, P. Erasenthiran, High speed sintering—early research into a new rapid manufacturing process, SFF Symposium, Austin, Texas, 2004, pp. 312-320.

[4] C.E. Majewski, B.S. Hobbs, N. Hopkinson, Effect of bed temperature and infra-red lamp power on the mechanical properties of parts produced using high-speed sintering, Virtual and Physical Prototyping 2(2) (2007) 103-110.

[5] A. Ellis, C.J. Noble, N. Hopkinson, High Speed Sintering: Assessing the influence of print density on microstructure and mechanical properties of nylon parts, Additive Manufacturing 1–4 (2014) 48-51.

[6] A. Ellis, L. Hartley, N. Hopkinson, Effect of Print Density on the Properties of High Speed Sintered Elastomers, Metallurgical and Materials Transactions A 46(9) (2015) 3883-3886.

[7] F. Norazman, N. Hopkinson, Effect of Sintering Parameters and Flow Agent on the Mechanical Properties of High Speed Sintered Elastomer, Journal of Manufacturing Science and Engineering 136(6) (2014) 061006-061006-6.

[8] H.R. Thomas, N. Hopkinson, P. Erasenthiran, High speed sintering—continuing research into a new rapid manufacturing process, SFF Symposium, Austin, Texas, 2006, pp. 682-691.

[9] A. Ellis, R. Brown, N. Hopkinson, The effect of build orientation and surface modification on mechanical properties of high speed sintered parts, Surface Topography: Metrology and Properties 3(3) (2015).

[10] C. Majewski, H. Zarringhalam, N. Hopkinson, Effect of the degree of particle melt on mechanical properties in selective laser-sintered Nylon-12 parts, Proceedings of the Institution of Mechanical Engineers, Part B: Journal of Engineering Manufacture 222(9) (2008) 1055-1064.

[11] P. Delfs, H.J. Schmid, Areal surface characterization of laser sintered parts for various process parameters, SFF 2017, Austin, Texas, 2017, pp. 2624 - 2631.

[12] L.S. Thomas, J.G. Timothy, S.U. John, The effect of process conditions on mechanical properties of laser-sintered nylon, Rapid Prototyping Journal 17(6) (2011) 418-423.

[13] E.C. Company, Technical Data Sheet - Amphora™ 3D Polymer SP1621 Natural, in: T.D.S.-A.T.D.P.S. Natural (Ed.) Eastman Chemical Company, 2018.